Surface Composition of Mars: Results from a New Atmospheric Compensation Technique Applied to TES.
L.E. Kirkland[1], K. C. Herr[2], J. Ward[3], E. R. Keim[2], J. H. Hackwell[2], J. M. McAfee[4], [1]Lunar and Planetary Institute, Houston, kirkland@lpi.usra.edu; [2]The Aerospace Corporation, kenneth.c.herr@aero.org; [3]Jet Propulsion Laboratory; [4]Los Alamos National Laboratory, mcafee_john_m@lanl.gov.

Introduction. Mapping the mineral composition of the Martian surface is a major goal of the NASA interplanetary program. Thermal infrared spectra returned by the Global Surveyor Thermal Emission Spectrometer (TES, ~6–50 μm) have been used to infer the composition of the surface silicates [1]. Unfortunately a significant region of this spectral signature lies beneath the intense 1100 cm^{-1} (9 μm) atmospheric dust absorption. This signature is further complicated by atmospheric CO_2, water vapor, and ice cloud absorptions.

Since the signatures of the surface silicates are weak, an accurate method of removing the atmospheric spectral information is required to study these underlying surface signatures. Two closely related methods of atmospheric retrieval have been attempted using TES spectra [2]. In order to provide a fresh look at the signatures of the Martian surface, we have explored a very different atmospheric retrieval process that has been used successfully on terrestrial hyperspectral data images. Here we compare the derived surface signature to previous results, and discuss implications for the derived surface composition.

Method. We use an In-Scene Atmospheric Compensation (ISAC) that was developed and tested using the airborne Spatially Enhanced Broadband Array Spectrograph System. SEBASS is a spectrometer (hyperspectral) that measures with uniquely high sensitivity (signal-to-noise ratio) over the 7.6–13.5 μm range in 128 bands [3].

Surface radiance propagates once through the atmospheric path. The atmosphere absorbs the surface radiance at characteristic frequencies, and also re-emits radiance at those frequencies. If reflected downwelling radiance is neglected, the radiance measured by TES (L_{OBS}) is approximated as [4]:

$$L_{OBS} = (\tau \cdot \varepsilon_S \cdot L_S) + L_{UP} \qquad (1)$$

where τ is the atmospheric transmission, ε_S is the surface emissivity, L_S is the surface blackbody radiance, and L_{UP} is the atmospheric re-emission. It may be rearranged as:

$$\varepsilon_S \cdot L_S = (L_{OBS} - L_{UP}) / \tau \qquad (2)$$

Thus we need to calculate the upwelling atmospheric radiance (L_{UP}) and the atmospheric transmission (τ), then use Equation 2 to compensate the spectra. [3] gives details of the calculation. Once $\varepsilon_S \cdot L_S$ is calculated, it is then converted to apparent emissivity(ε_A) using:

$$\varepsilon_A = \varepsilon_S \cdot L_S / L_{BB} \qquad (3)$$

where L_{BB} is the blackbody curve calculated for the brightness temperature from the L_S radiance in the 7.75 μm region [5,6].

Fig. 1 shows the calculated atmospheric transmission spectrum and a surface signature derived for Syrtis Major. The surface signature is subtle compared to the transmission spectrum. This illustrates the importance of a very high quality atmospheric compensation.

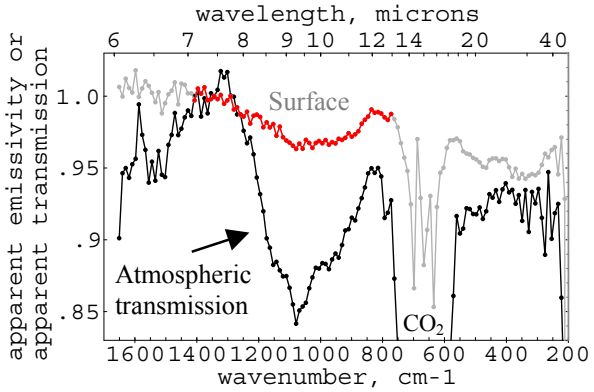

Figure 1: The atmospheric transmission spectrum is in apparent transmission and the surface spectrum in apparent emissivity, both with respect to 7.75 μm. The surface spectrum shows the full spectral range measured by TES, but not all wavelengths sound the surface because of strong atmospheric bands. Atmospheric CO_2, aerosol dust, and water vapor cause the strongest atmospheric transmission features.

Data used. The region sampled was -10–30° latitude and 285–320° longitude (western Syrtis and eastern Arabia). We used mapping phase TES data (cdroms 134–139, TES orbits 3888–4207). After examining all wavelengths, we limited the wavelength range used from ~1400 to 750 cm^{-1} (61 points). We dropped ~750–600 cm^{-1} because of the strong 667 cm^{-1} CO_2 gas absorption. The 1971 IRIS spectra typically show a much more distinct 20 μm band than TES data [7], so we approach wavenumbers <600 cautiously until the reason for this difference can be understood. Further, we limited data used to a peak-to-peak signal-to-noise ratio (SNR) above 20 (~100 r.m.s. SNR) at 270 K [6], which here excluded wavenumbers >1400.

Observations. Fig. 2 shows TES spectra that have had ISAC applied and averaged to increase the SNR. The dark region spectrum (average albedo=0.10) is from central Syrtis Major. The brighter region spectrum (average albedo=0.27) is from eastern Arabia. Brighter regions have a sloping continuum at higher wavenumbers, are relatively flat in the 9 μm region, and have an emissivity trough near 850 cm^{-1}. Dark region spectra have a relatively flat continuum at shorter wavelengths and a broad, U-shaped 9 μm band.

Discussion. We interpret the ~825 cm^{-1} feature in

the brighter region spectra as a silicate transparency feature [8]. A sloping continuum at higher wavenumber, flat 9 µm region, transparency feature, and higher albedo are all consistent with finely particulate silicates [e.g. 8,9]. For darker region spectra, the relatively flat continuum at >1250 cm^{-1}, broad 9 µm band, and low albedo are all consistent with coarse silicate material.

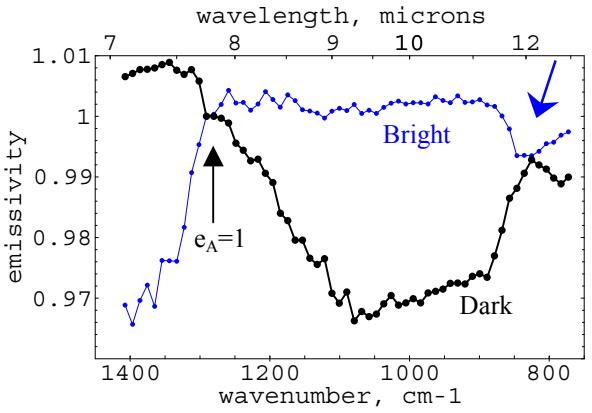

Figure 2: The blue trace is an average of 746 spectra of a typical brighter region (~415 km x 850 km), centered at 14°N latitude, 313° longitude. The right arrow indicates the possible transparency feature. The black trace is 528 averaged spectra of a dark region (~1190 km x 290 km) centered at 10°N latitude, 293° longitude. Spectra are shown in apparent emissivity (e_A) with respect to 7.75 µm (left arrow).

TES-team method. The first step in the TES-team atmospheric compensation is to assume that large bright regions are blackbodies [2]. Next, they average many (>100) spectra measured of a bright region, and assume it represents purely an atmospheric signature. The signature is scaled either to apparent opacity using a method they label radiative transfer, or to apparent emissivity. The bright region spectrum and a water ice cloud spectrum are then scaled to signatures measured of other regions using linear mixture modeling. The residual is assumed to be the surface signature.

Fig. 3 shows the Fig. 2 dark region spectrum, and the derived surface signatures from [1]. The ISAC-derived spectrum is from a "Surface Type 1" (basaltic) region in [1], and the 9 µm bands are broadly consistent. However, the location of the ISAC-derived Christiansen peak near 1300 cm^{-1} is more consistent with the TES-team "Surface Type 2" andesitic spectrum.

Differences. ISAC differs from the TES team's method in that ISAC does not assume bright regions are blackbodies to derive the atmospheric signature.

Our results differ in two main areas. First, the brighter regions we examined are not blackbodies, but their signatures are consistent with fine-grained silicates. If this result is correct, an assumption that bright regions are blackbodies will be a source of error for the derived surface signature in [1]. This would also account for the failure of their method at shorter wavelengths. Their derived surface signature ends at 1301 cm^{-1} (e.g. Fig. 3) where the ISAC-derived brighter region emissivity begins decreasing sharply.

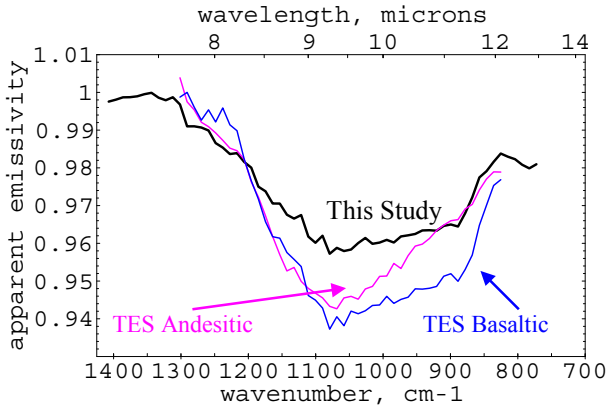

Figure 3: The black trace shows the Fig. 4 dark region spectrum. The TES-team data were kindly provided by Dr. J. Bandfield for the andesitic and basaltic type regions of [1].

Second, the derived surface signatures have different Christiansen peaks. Increasing silica content or weathering products can shift this shoulder to shorter wavelength [10]. Thus the "andesitic" signature has a shorter wavelength peak than the "basaltic" signature (Fig. 3). However, the "andesitic" signature stops before the peak is defined, and the "basaltic" signature stops before it is well-defined (Fig 3). Thus the shoulder and peak location may also be affected by different peak values used for the conversion to apparent emissivity. This illustrates the critical importance of determining the surface signature to a shorter wavelength.

Conclusions. One strength of ISAC is that it does not require a single region that is a blackbody at all wavelengths to derive the atmospheric signature. One weakness is that ISAC was developed for very high signal-to-noise ratio data, and this makes it difficult to apply to TES. The best result may come from a combination of the two methods. ISAC can be used to determine the bright region signature and for spot-testing, and then apply the TES-team method more globally. The TES-team method should also be tested using terrestrial hyperspectral data. The atmospheric spectral contrast is so much stronger than the surface that even small imperfections in the compensation will map into the derived surface composition. Testing is important to determine the uncertainties in the current methods.

References. [1] Bandfield J.L. et al. (2000) *Science 287*, 1626. [2] Smith M.D. et al. (2000), *JGR 105*, 9589. [3] Kirkland L.E. et al. (2001) *accepted Rem. Sens. Env.*, preprint: www.lpi.usra.edu/science/kirkland. [4] Schott J.R. (1997) *Remote Sensing,* Oxford UP. [5] Conel J. E. (1969) *JGR 74*, 1614. [6] Kirkland L.E. et al. (2001) *Appl. Optics 40*, 4852. [7] Kirkland L.E. et al. (2001) *LPSC XXXII abs. 1864*. [8] Salisbury J.W. and L.S. Walter. (1989) *JGR 94*, 9192. [9] Salisbury J.W. et al. (1991) *Infrared (2.1–25 micron) Spectra of Minerals,* JHU Press. [10] Logan L.M. et al. (1973) *JGR 78*, 4983.